A spray-flamelet formulation using an effective composition-space variable

By B. Franzelli, A. Vié AND M. Ihme

1. Motivation and objectives

Motivated by the utilization of liquid fuels for transportation and propulsion systems, considerable progress has been made in the analysis of spray flames (Faeth 1983; Borghi 1996*a*; Sirignano 2010; Jenny *et al.* 2012; Sirignano 2014; Sanchez *et al.* 2014). While gaseous diffusion flames are characterized by the competition between scalar mixing and chemistry, spray flames require the continuous supply of gaseous fuel via evaporation and transport to the reaction zone to sustain combustion. Because of this complexity, the investigation of spray flames in canonical combustion configurations, such as mixing layers and counterflow flames, represents a viable approach to obtain physical insight into the behavior of spray flames (Continillo & Sirignano 1990; Hollmann & Gutheil 1998; Lerman & Greenberg 2010).

Counterflow spray flames have been the subject of intensive research, and considerable numerical and experimental studies have been performed by considering laminar conditions (Continillo & Sirignano 1990; Li *et al.* 1992; Darabiha *et al.* 1993; Massot *et al.* 1998; Gutheil & Sirignano 1998; Gutheil 2005; Watanabe *et al.* 2007). Theoretical investigations provided understanding about underlying physical processes, involving flame stabilization and extinction processes of spray flames (Lerman & Greenberg 2010; Greenberg & Sarig 1993; Dvorjetski & Greenberg 2002, 2009). More recently, bistable flame structures of laminar flames were considered for examining the bifurcation in three-dimensional turbulent counterflow spray flames (Vié *et al.* 2014*a*). As such, the characterization of the structure of spray flames is of fundamental relevance for a wide range of operating regimes.

In the context of laminar gaseous diffusion flames, the flame structure is typically examined in composition space by introducing the gaseous mixture fraction Z_g as an independent variable (Peters 1984). This conserved scalar is defined with respect to the gaseous mixture composition and provides a unique mapping between physical and composition space, thereby eliminating the explicit dependence on the spatial coordinate. This mixture-fraction formulation is also used in turbulent combustion models, enabling the representation of the turbulence-chemistry interaction through presumed probability density function models (Borghi 1996*b*; Demoulin & Borghi 2000). Another significant advantage of a mixture-fraction representation arises from the computationally efficient solution of the resulting flamelet equations in composition state. Therefore, extending the mixture-fraction concept to spray flames is desirable and enables to be utilized the analysis tools that have been developed for gaseous flame.

Unfortunately, this extension is non-trivial since the classical gaseous mixture-fraction definition loses its monotonicity due to evaporation (Olguin & Gutheil 2014*a*; Vié *et al.* 2014*b*). With the exception of pre-vaporized flames and other simplifying assumptions, the structure of spray flames cannot be studied in the classical mixture-fraction space. Because of this, spray flames are commonly solved in physical space and then transformed

into Z_g-space; for example, by separating the purely gaseous region of the flame from the evaporation zone (Olguin & Gutheil 2014*a*; Bilger 2011; Olguin & Gutheil 2014*b*). Although feasible, this approach introduces undesirable model complexities. Specifically, commonly employed tabulation methods require the construction of two distinct tables that distinguish the purely gaseous region and the two-phase zone (Hollmann & Gutheil 1998; Olguin & Gutheil 2014*a*). Moreover, due to its non-monotonicity, the classical gaseous definition cannot be used to solve the spray flamelet equations in composition space. By addressing these issues, the objective of this work is to propose a new composition-space variable that enables the description of spray flames. The key idea for this formulation consists in identifying a unique and monotonic representation of a mixing-describing coordinate for spray flames. This new coordinate, referred to as effective composition variable η, is useful both for analyzing the flame structure and for effectively solving the corresponding spray flamelet equations. In addition, the effective composition variable η is defined in such a way that it extends the classical flamelet formulation for gaseous diffusion systems (Peters 1984; Williams 1985; Liñán 1974; Poinsot & Veynante 2012), thereby ensuring consistency.

The remainder of this work is organized as follows. The spray-flamelet equations in physical space are presented in Section 2, together with the definition of the effective composition variable. The versatility of this formulation is demonstrated by considering in Section 3 the analysis of the spray-flame structure in composition space. The spray-flamelet equations in η-space are formulated in Section 4. Comparisons of simulation results with solutions obtained in physical space are performed. It is shown that the proposed formulation is able to reproduce the spray-flame structure for different values of the strain rate and the droplet diameter.

2. Governing equations

In the present work, we consider a mono-disperse spray flame in a counterflow configuration, and the governing equations are formulated in a Eulerian framework. In this configuration, fresh air is injected against a stream consisting of a fuel spray and pure air. Consistent with the classical analysis of gaseous flames, the following assumptions are invoked (Peters 1984; Williams 1985; Poinsot & Veynante 2012): (i) steady-state solution and low-Mach number limit, (ii) unconfined flame and constant thermodynamic pressure, (iii) single-component fuel, (iv) unity Lewis number, equal but not necessarily constant diffusivities for all chemical species and temperature: $D_k = D_{th} = \lambda/(\rho c_p) \equiv D$ (Ficks' law without velocity correction is used for diffusion velocities (Poinsot & Veynante 2012)), (v) calorically perfect gas $c_{p,k} = c_p = \text{constant}$, (vi) a constant strain rate is assumed $u = -ax$, (vii) constant thermo-diffusive properties with $\rho D = 2 \times 10^{-5}$ kg/(m s) and $c_p = 1300$ J/(kg K), (viii) equal gas and liquid velocities †, (ix) a simplified d^2-model for evaporation, with fixed droplet temperature $T_l = T_b$, where T_b is the boiling temperature of the fuel species. Consequently, the evaporation model is

$$\dot{m} = 2\pi n_l d \rho D \ln\left[\frac{c_p}{L_v}(T - T_l)\right] \mathcal{H}(T - T_l), \tag{2.1}$$

$$q = L_v, \tag{2.2}$$

† This assumption is valid for small Stokes-number droplets based on the gaseous flow strain rate $\mathrm{St}_d = a\tau_d$ (where $\tau_d = \rho_l d^2/(18\mu)$ is the particle relaxation time (Maxey & Riley 1983)).

where n_l is the liquid droplet number density, $\mathcal{H}(\cdot)$ is the Heaviside function, $\dot{m}$ is the total mass vaporization rate and q is the heat transfer ratio from the gas to each droplet. The liquid fuel properties for kerosene are boiling temperature $T_b = 478$ K and latent heat of evaporation $L_v = 289.9$ kJ/kg.

In this context, note that the composition variable and formulation proposed in this paper are not restricted to these assumptions and can equally be extended in analogy to the gaseous theory.

Under these assumptions, we introduce the transport equations for the gaseous phase (species mass fractions Y_k and temperature T) and the liquid phase (the liquid-to-gas mass ratio $Z_l = \frac{\alpha_l \rho_l}{\rho}$ and the individual droplet mass m_d) in physical space (Continillo & Sirignano 1990)

$$-ax\frac{\mathrm{d}Y_k}{\mathrm{d}x} = \rho D\frac{\mathrm{d}^2 Y_k}{\mathrm{d}x^2} + \dot{m}(\delta_{kF} - 1) + \dot{\omega}_k \ , \tag{2.3a}$$

$$-ax\frac{\mathrm{d}T}{\mathrm{d}x} = \rho D\frac{\mathrm{d}^2 T}{\mathrm{d}x^2} + \dot{m}\left(T_l - T - \frac{L_v}{c_p}\right) + \dot{\omega}_T \ , \tag{2.3b}$$

$$-ax\frac{\mathrm{d}Z_l}{\mathrm{d}x} = -\dot{m}(Z_l + 1) \ , \tag{2.3c}$$

$$-ax\frac{\mathrm{d}m_d}{\mathrm{d}x} = -\dot{m}\frac{\rho}{n_l} \ , \tag{2.3d}$$

where ρ is the density, calculated from the species mass fractions. The production rate of species k is denoted by $\dot{\omega}_k$, $\dot{\omega}_T = -\sum_{k=1}^{N_s} \dot{\omega}_k W_k h_k / c_p$ is the heat-release rate, h_k is the sensible and chemical enthalpy of species k, c_p is the heat capacity of the gaseous mixture, δ_{ij} is the Kronecker delta, and N_s is the total number of species. Subscript l is used to identify quantities of the liquid phase and the subscript F refers to the fuel. $\alpha_l = n_l \pi d^3/6$ is the liquid volume fraction, $m_d = \rho_l \pi d^3/6$ is the individual droplet mass, ρ_l is the liquid density, and d is the droplet diameter.

2.1. *A new monotonic mixing-describing coordinate*

In Vié *et al.* (2014*b*), the authors investigate the use of several definitions for the mixture fraction and show that the simple use of either the gaseous mixture fraction or the total mixture fraction (gaseous+liquid carbon atoms) is insufficient to build a well-defined monotonic mixing-describing coordinate. In the present work, we introduce a strictly monotonic effective composition variable

$$(\mathrm{d}\eta)^2 = (\mathrm{d}Z_g)^2 + (\mathrm{d}Z_l)^2 \ , \tag{2.4}$$

which is defined as the arc length in (Z_g, Z_l)-space, where Z_g is the classical gaseous non-normalized mixture fraction (Bilger *et al.* 1990). By definition, the quantity η increases monotonically, thereby providing a unique identification of the normal to the flame surface. Moreover, this effective composition variable reduces to the classical gaseous mixture fraction expression in the absence of a liquid phase, guaranteeing the consistency with the single-phase flamelet formulation. In the following, we investigate the use of this definition to describe the structure of spray flames.

3. Analysis of spray flame structure

This work considers a counterflow configuration, which consists of two opposed injection slots that are separated by a distance $L = 0.02$ m along the x_1-direction, see

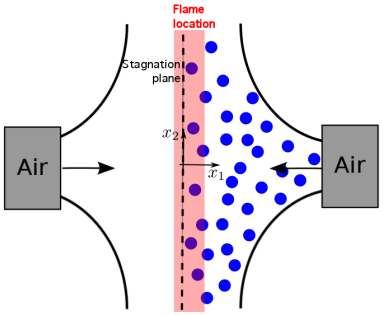

FIGURE 1: Schematic of the laminar counterflow spray flame.

Figure 1. On the fuel side, a mono-disperse kerosene ($C_{10}H_{20}$) spray is injected with air. On the oxidizer side, pure air is injected. Similar to the works by Dvorjetski & Greenberg (2002) and Lerman & Greenberg (2010), the gaseous flow field is assumed to be described by a constant strain rate†: $u = -ax$ and $v = ay$. Compared to gaseous flames, the boundary conditions are not imposed at infinity in order to take into account the effect of the evaporation on the mixing and reaction‡. The following gaseous boundary conditions are imposed at both sides: $T^0 = 600$ K, $Y^0_{O_2} = 0.233$, $Y^0_{N_2} = 0.767$. For the liquid phase at the spray side, the liquid-to-gas mass fraction is $Z^0_l = 0.2$. In the present study, we examine effects of the droplet diameter of the injected spray, d^0, and the strain rate, a, on the flame structure. To focus on the coupling between mass transfer, mixing and reaction processes, approximations on the evaporation model, the liquid velocity and temperature have been invoked for the numerical solution of the spray flame equations. The reaction chemistry is described by a two-step six-species mechanism that was developed for kerosene/air flames under the assumption of unity Lewis numbers (Franzelli *et al.* 2010).

3.1. *Flame structure in effective composition space*

The counterflow spray-flame equations, Eqs. (2.3) are solved in physical space and the effective composition variable η is used to analyze the flame structure for different values of d^0 and a. Results for different initial droplet diameters and strain rates are illustrated in Figures 2 and 3, showing the solution in physical space (left) and in effective composition space (middle). The location separating the evaporation and mixing regions is indicated by the vertical blue line.The region where diffusion affects the results is presented in gray in all figures.

3.1.1. *Effects of droplet diameter on spray-flame structure*

Results for a constant strain rate of $a = 100$ s^{-1} and three different initial droplet diameters of $d^0 = \{20, 40, 80\}$ μm are presented in Figure 2. For $d^0 = 20$ μm (Figure 2(a)), the liquid fuel fully evaporates before reaching the flame reaction zone, and the high-

† Despite the fact that this assumption is not exact for variable density flows, it reduces the computational complexity of the counterflow while keeping the main physics, and it is often used as a simplified model for two-phase flame analysis (Lerman & Greenberg 2010; Dvorjetski & Greenberg 2002).

‡ For $L \to \infty$, the pre-evaporated case is retrieved, as the evaporation takes place before reaching the flame/mixing region.

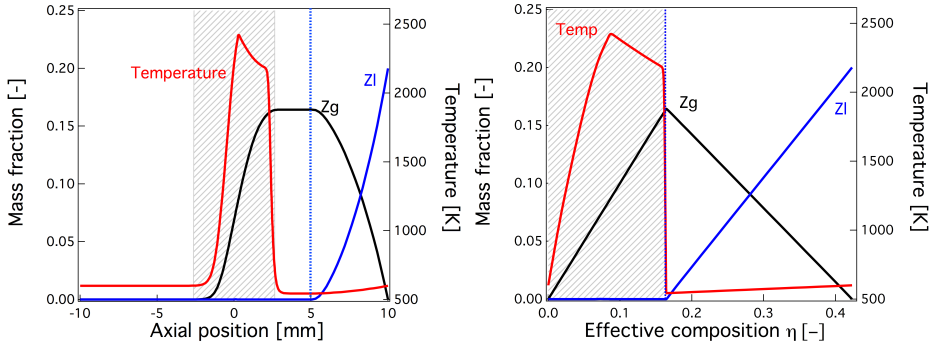

(a) Initial droplet diameter: $d^0 = 20$ μm.

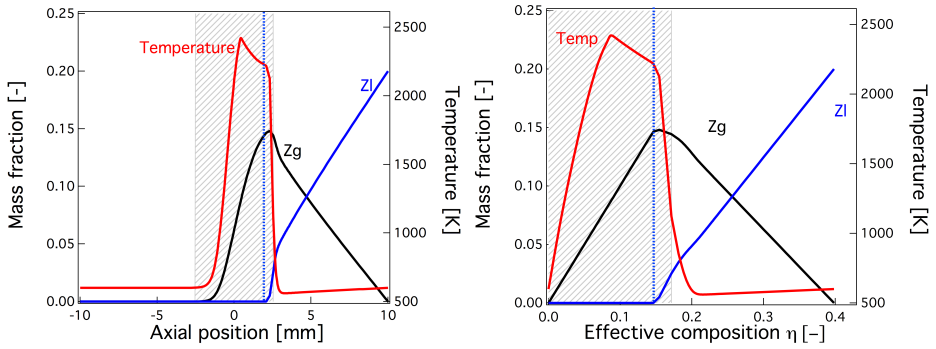

(b) Initial droplet diameter: $d^0 = 40$ μm.

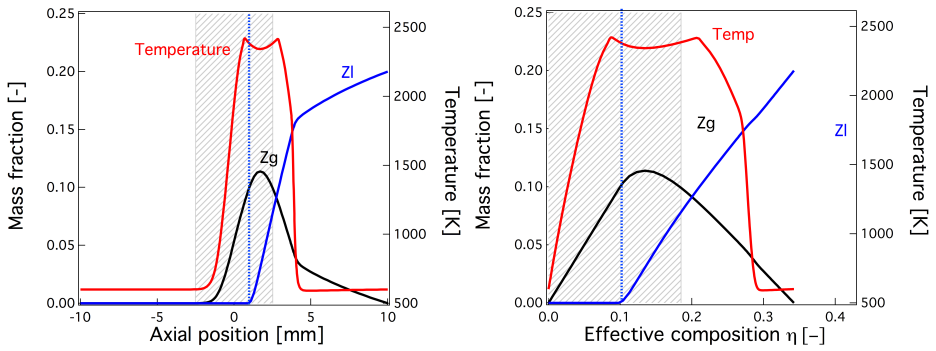

(c) Initial droplet diameter: $d^0 = 80$ μm.

FIGURE 2: Flame structure obtained from the solution in physical space for $a = 100$ s^{-1} as a function of different initial droplet diameters d^0: solution in x-space (left) and in η-space (right); the gray area corresponds to the diffusion zone; the blue vertical line separates the spray side from the gas side.

temperature region is confined to the gas region of the flame. By considering the budget analysis, it can be seen that the diffusion contribution on the spray side is negligible.

By increasing the initial droplet diameter to $d^0 = 40$ μm (Figure 2(b)), it can be seen that a small amount of liquid fuel reaches the preheat zone of the flame. The evaporation is not separated from the diffusion region. As shown in the right panel of Figure 2(b), the

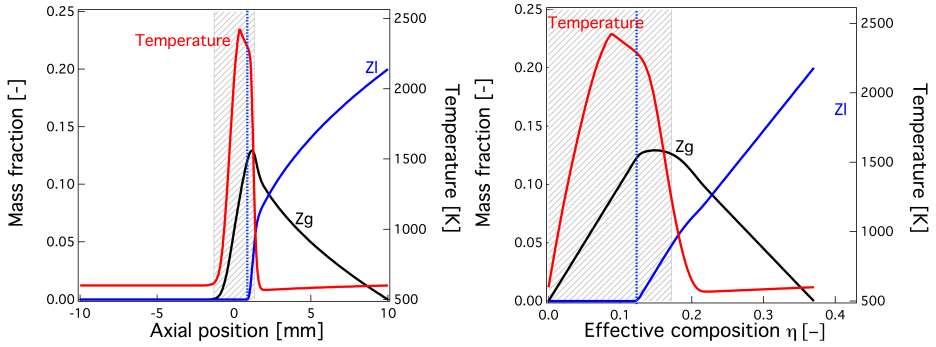

(a) Strain rate: $a = 200\ \mathrm{s}^{-1}$.

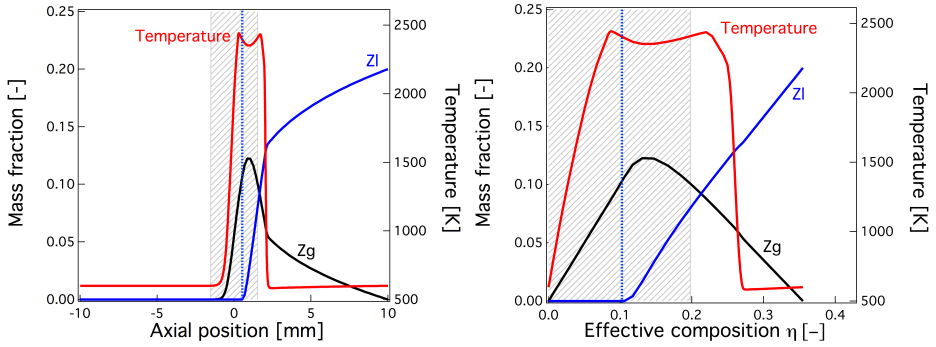

(b) Strain rate: $a = 400\ \mathrm{s}^{-1}$.

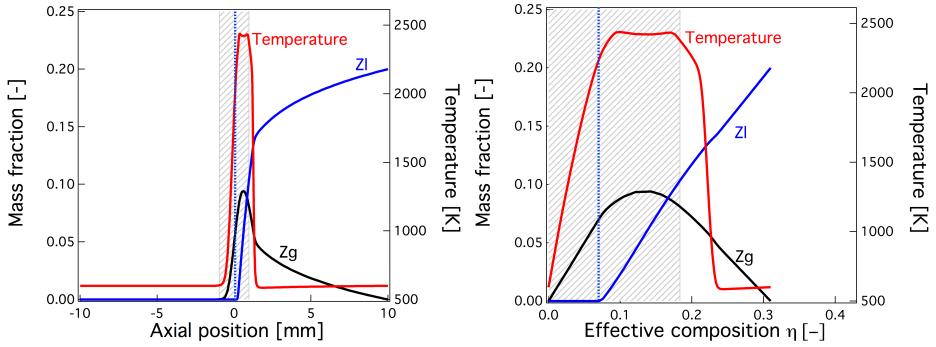

(c) Strain rate: $a = 600\ \mathrm{s}^{-1}$.

FIGURE 3: Flame structure obtained from the solution in physical space for $d^0 = 40\ \mu$m as a function of different strain rates a: solution in x-space (left) and in η-space (right); the gray area corresponds to the diffusion zone; the blue vertical line separates the spray side from the gas side.

diffusive part of the budget can no longer be neglected close to the maximum value of Z_g, and the maximum values for η and Z_g are smaller compared to the case for $d^0 = 20\ \mu$m.

For the case with $d^0 = 80\ \mu$m (Figure 2(c)) liquid fuel is penetrating into the reaction zone, and a high-temperature region and a second heat-release region on the spray side can be observed. This complex flame structure is clearly visible in the η-space. Moreover,

as evidenced by the overlap between the gray region and the liquid volume fraction Z_l, as well as by the budget analysis, both diffusive and evaporative contributions are mixed.

Considering the η-space, the effect of the droplet diameter on the flame structure is clearly identified. For all three cases considered, the first temperature peak is located on the gas side at stoichiometric conditions. However, with increasing initial droplet diameter, a second temperature peak is formed on the spray side, which identifies the transition from a single-reaction to a double-reaction flame structure for large droplets (Gutheil 2005; Vié *et al.* 2014*a*). By increasing the droplet diameter, diffusion effects become increasingly important in the spray region, and the diffusive processes overlap with evaporation.

3.1.2. *Effects of strain rate on spray-flame structure*

Results for different strain rates $a = \{200, 400, 600\}$ s^{-1} and fixed initial droplet diameter of $d^0 = 40$ μm are illustrated in Figure 3. Compared to the results in physical space for a lower strain rate $a = 100$ s^{-1} (Figure 2(b)), the flame structure in Figure 3(a) is confined to a narrow region for $a = 200$ s^{-1}. However, the representation of the flame structure with respect to the effective composition variable η provides a clear description of the different regions that are associated with the heat release and diffusion effects.

The flame structure for a strain rate of $a = 400$ s^{-1} is shown in Figure 3(b). For this condition, a double-flame structure is observed in which the primary heat-release zone is formed on the spray side and the vaporized fuel is consumed in a secondary reaction zone on the gaseous side of the flame. The different reaction zones are conveniently identified in composition space, and the budget analysis provides a clear description of the contributions arising from a balance between diffusion and advection in the absence of evaporation effects.

By further increasing the strain rate to a value of $a = 600$ s^{-1} a high-temperature region is observed on the spray side (Figure 3(c)). However, compared to the case with $a = 400$ s^{-1} the two heat-release zones are closer without exhibiting a significant reduction in temperature. At this condition, the flame on the gas side is highly strained, leading to a reduction of the maximum temperature (from 2400 to 2000 K), and both temperature peaks are located on the spray side. In comparison, the maximum temperature on the spray side is less affected by variations in strain rate.

4. Derivation of spray flamelet equations in effective composition space

One of the main motivations for introducing the monotonic composition-space variable η is to enable the direct solution of Eq. (2.3) in composition space.

Rewriting Eq. (2.3) by introducing the effective composition space variable η and by assuming a constant pressure along the η-direction, we obtain the complete spray flamelet

equations

$$\Xi_\eta^\dagger \frac{\mathrm{d}Y_k}{\mathrm{d}\eta} = \frac{\rho\chi_\eta}{2}\frac{\mathrm{d}^2 Y_k}{\mathrm{d}\eta^2} + (\delta_{kF} - Y_k)\dot{m} + \dot{\omega}_k \ , \tag{4.1a}$$

$$\Xi_\eta^\dagger \frac{\mathrm{d}T}{\mathrm{d}\eta} = \frac{\rho\chi_\eta}{2}\frac{\mathrm{d}^2 T}{\mathrm{d}\eta^2} + \dot{m}\left(T_l - T - \frac{L_v}{c_p}\right) + \dot{\omega}_T \ , \tag{4.1b}$$

$$\Xi_\eta \frac{\mathrm{d}Z_l}{\mathrm{d}\eta} = -\dot{m}\left(1 + Z_l\right) \ , \tag{4.1c}$$

$$\Xi_\eta \frac{\mathrm{d}m_d}{\mathrm{d}\eta} = -\dot{m}\frac{\rho}{n_l} \ , \tag{4.1d}$$

with

$$\Xi_\eta = \mathrm{sgn}(u_\eta)\left\{\left(\frac{\mathrm{d}Z_g}{\mathrm{d}\eta}\frac{\rho D}{2}\frac{\mathrm{d}}{\mathrm{d}\eta}\left(\frac{\chi_\eta}{2D}\right) + \frac{\rho\chi_\eta}{2}\frac{\mathrm{d}^2 Z_g}{\mathrm{d}\eta^2} + (1 - Z_g)\dot{m}\right)^2 + \left(\dot{m}\left(1 + Z_l\right)\right)^2\right\}^{1/2} , \tag{4.2a}$$

$$\Xi_\eta^\dagger = \Xi_\eta - \frac{\rho D}{2}\frac{\mathrm{d}}{\mathrm{d}\eta}\left(\frac{\chi_\eta}{2D}\right) \ , \tag{4.2b}$$

and χ_η is the scalar dissipation of the variable η

$$\chi_\eta = 2D\frac{\mathrm{d}\eta}{\mathrm{d}x}\frac{\mathrm{d}\eta}{\mathrm{d}x} \ . \tag{4.3}$$

Note that $\Xi_\eta^\dagger$ is equal to zero on the gas side.

To confirm consistency, it can be seen that the spray-flamelet formulation Eq. (4.1) reduces to the classical gaseous mixture-fraction formulation in the absence of a liquid phase. Olguin & Gutheil (2014*a*) proposed a spray-flamelet formulation in Z_g-composition space, and evaluated the contribution of each term from the solution of the counterflow spray flame in physical space. In the present work, the spray-flamelet equations are directly solved as a function of the effective composition space η. The only unclosed terms in the spray-flamelet equations are χ_η and $\mathrm{sgn}(u_\eta) = -\mathrm{sgn}(x)$. The development of such closures has been addressed in Franzelli *et al.* (2014). In order to assess the consistency of the composition-space formulation through direct comparisons with spray-flame solutions from the physical space, the spray-flamelet equations Eq. (4.1) are here solved using expressions for χ_η and $\mathrm{sgn}(u_\eta)$ that are directly evaluated from the physical-space spray-flame solutions.

The solutions obtained in physical space using 400 mesh points with adaptive refinement (solid lines) and in composition space with 100 mesh points with equidistant grid spacing (symbols) are compared in Figure 4. The operating conditions correspond to the case discussed in Section 3 ($d_0 = 40$ μm and $a = 100$ s^{-1}). The excellent agreement between both solutions is a direct verification of the newly proposed spray-flamelet formulation for providing a viable tool for the flame-structure representation and as a method for solving the spray-flamelet equations in composition space.

5. Conclusions

A composition variable is proposed to study the structure of spray flames in composition space in analogy with the classical theory for purely gaseous diffusion flames. Unlike previous definitions (Olguin & Gutheil 2014*a*; Luo *et al.* 2014) that have been

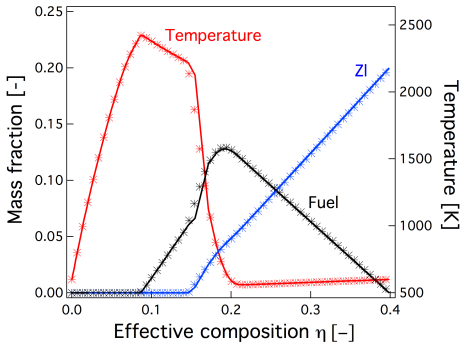

FIGURE 4: Comparison of spray-flame structure for $d^0 = 40\ \mu m$ and $a = 100\ \mathrm{s}^{-1}$ obtained from the solution in physical space (symbols) and in η-composition space (solid lines) where χ_η is extracted from the x-space solution.

used to describe a mixture-fraction variable, the newly proposed effective composition variable η is monotonic, thereby enabling the representation and analysis of spray flame structures in composition space. Furthermore, as this new definition is also based on the liquid-to-gas mass fraction, it can also capture the evolution of the disperse phase even if no evaporation occurs, which is not the case for purely gaseous-based definitions.

This new composition space is used to analyze counterflow spray flames simulated in physical space, showing its ability to represent the spray-flame structure. By using the effective composition variable, a flamelet formulation is derived and solved, showing the consistency of our formulation with the physical space solution. From these flamelet equations arises the necessity of closures for the scalar dissipation rate and the slip velocity. This formulation represents a theoretical tool for the asymptotic analysis of spray flames (Lerman & Greenberg 2010) in composition space. This formulation can be considered as the theoretical foundation for one-dimensional spray flamelet formulations (Hollmann & Gutheil 1998; Martinez-Ruiz *et al.* 2013) for turbulent combustion models. The formulation can be extended to polydisperse flow field, by using for instance a multifluid formulation for the droplet phase (Laurent & Massot 2001).

Acknowledgments

The authors gratefully acknowledge financial support from SAFRAN, and through NASA with Award Nos. NNX14CM43P and NNM13AA11G. Helpful discussions with Prof. Sirignano on the spray-flamelet formulation are appreciated.

REFERENCES

BILGER, R. W. 2011 A mixture fraction framework for the theory and modeling of droplets and sprays. *Combust. Flame* **158**, 191–202.

BILGER, R. W., STARNER, S. H. & KEE, R. J. 1990 On reduced mechanisms for methane-air combustion in nonpremixed flames. *Combust. Flame* **80** (2), 135–149.

BORGHI, R. 1996*a* Background on droplets and sprays. In *Combustion and turbulence in two phase flows, Lecture Series 1996-02*. Von Karman Institute for Fluid Dynamics.

BORGHI, R. 1996*b* The links between turbulent combustion and spray combustion and

their modelling. In *8th International Symposium on Transport Phenomena in Combustion*, pp. 1–18.

Continillo, G. & Sirignano, W. A. 1990 Counterflow spray combustion modeling. *Combust. Flame* **81**, 325 – 340.

Darabiha, N., Lacas, F., Rolon, J. C. & Candel, S. 1993 Laminar counterflow spray diffusion flames: A comparison between experimental results and complex chemistry calculations. *Combust. Flame* **95**, 261–275.

Demoulin, F. & Borghi, R. 2000 Assumed PDF modeling of turbulent spray combustion. *Combust. Sci. Tech.* **158**, 249–271.

Dvorjetski, A. & Greenberg, J. B. 2002 Steady-state and extinction analyses of counterflow spray diffusion flames with arbitrary finite evaporation rate. *Combust. Sci. Tech.* **174**, 187–208.

Dvorjetski, A. & Greenberg, J. B. 2009 Analysis of steady state polydisperse counterflow spray diffusion flames in the large stokes number limit. *Proc. Combust. Inst.* **32**, 2205–2214.

Faeth, G. M. 1983 Evaporation and combustion of sprays. *Prog. Energy Comb. Sci.* **9**, 1–76.

Franzelli, B., Riber, E., Sanjosé, M. & Poinsot, T. 2010 A two-step chemical scheme for large eddy simulation of kerosene-air flames. *Combust. Flame* **157**, 1364–1373.

Franzelli, B., Vié, A. & Ihme, M. 2014 A new composition space based on a monotonic mixing-describing variable for the flamelet formulation of spray flames. *Combust. Flame* , Under Review.

Greenberg, J. B. & Sarig, N. 1993 Coupled evaporation and transport effects in counterflow spray diffusion flames. *Combust. Sci. Tech.* **92**, 1–33.

Gutheil, E. 2005 Multiple solutions for structures of laminar counterflow spray flames. *Prog. Comput. Fluid Dyn.* **5**, 414–419.

Gutheil, E. & Sirignano, W. A. 1998 Counterflow spray combustion modeling with detailed transport and detailed chemistry. *Combust. Flame* **113**, 92–105.

Hollmann, C. & Gutheil, E. 1998 Diffusion flames based on a laminar spray flame library. *Combust. Sci. Tech.* **135**, 175–192.

Jenny, P., Roekaerts, D. & Beishuizen, N. 2012 Modeling of turbulent dilute spray combustion. *Prog. Energy Comb. Sci.* **38**, 846–887.

Laurent, F. & Massot, M. 2001 Multi-fluid modeling of laminar poly-dispersed spray flames: origin, assumptions and comparison of the sectional and sampling methods. *Combust. Theory and Modelling* **5**, 537–572.

Lerman, S. & Greenberg, J. B. 2010 Spray diffusion flames - an asymptotic theory. *Atomization and Sprays* **20**, 1047–1064.

Li, S. C., Libby, P. A. & Williams, F. A. 1992 Experimental and theoretical studies of counterflow spray diffusion flames. In *24th Symp. (Int.) on Combustion*, pp. 1503–1512. The Combustion Institute, Pittsburgh.

Liñán, A. 1974 The asymptotic structure of counterflow diffusion flames for large activation energies. *Acta Astronautica* **1**, 1007–1039.

Luo, K., Jianren, F. & Cen, K. 2014 New spray flamelet equations considering evaporation effects in the mixture fraction space. *Fuel* **103**, 1154–1157.

Martinez-Ruiz, D., Urzay, J., Sánchez, A. L., Liñán, A. & Williams, F. A.

2013 Dynamics of thermal ignition of spray flames in mixing layers. *J. Fluid Mech.* **734**, 387–423.

Massot, M., Kumar, M., Smooke, M. D. & Gomez, A. 1998 Spray counterflow diffusion flames of heptane: Experiments and computations with detailed kinetics and transport. *Proc. Combust. Inst.* **27**, 1975–1983.

Maxey, M. & Riley, J. 1983 Equation of motion for a small rigid sphere in a non uniform flow. *Phys. Fluids* **26**, 2883–2889.

Olguin, H. & Gutheil, E. 2014*a* Influence of evaporation on spray flamelet structures. *Combust. Flame* **161**, 987–996.

Olguin, H. & Gutheil, E. 2014*b* Theoretical and numerical study of evaporation effects in spray flamelet model. In *Experiments and Numerical Simulations of Turbulent Combustion of Diluted Sprays* (ed. B. Merci & E. Gutheil), pp. 79–106. Springer.

Peters, N. 1984 Laminar diffusion flamelet models in non-premixed turbulent combustion. *Prog. Energy Comb. Sci.* **10**, 319–339.

Poinsot, T. & Veynante, D. 2012 *Theoretical and Numerical Combustion,* 3rd ed.

Sanchez, A. L., Urzay, J. & Liñan, A. 2014 The role of separation of scales in the description of spray combustion. *Proc. Combust. Inst.* **35**, In Press.

Sirignano, W. A. 2010 *Fluid dynamics and transport of droplets and sprays, 2nd ed.,* Cambridge University Press.

Sirignano, W. A. 2014 Advances in droplet array combustion theory and modeling. *Prog. Energy Comb. Sci.* **42**, 54–86.

Vié, A., Franzelli, B., Gao, Y., Lu, T., Wang, H. & Ihme, M. 2014*a* Analysis of segregation and bifurcation in turbulent spray flames: a 3d counterflow configuration. *Proc. Combust. Inst.* **35**, In Press.

Vié, A., Franzelli, B., Ihme, M., Fiorina, B. & Darabiha, N. 2014*b* On the description of spray flame structure in the mixture fraction space. *Annual Research Briefs,* Center for Turbulence Research, Stanford University, pp. 93–106.

Watanabe, H., Kurose, R., Hwang, S. M. & Akamatsu, F. 2007 Characteristics of flamelets in spray flames formed in a laminar counterflow. *Combust. Flame* **148**, 234–248.

Williams, F. A. 1985 *Combustion Theory*. Benjamin Cummings.